Supplementary Information

Photoelectrochemical Oxidation of a Turn-On Fluorescent Probe Mediated by a Surface Mn^{II} Catalyst Covalently Attached to TiO_2 Nanoparticles

Alec C. Durrell, Gonghu Li,[†] Matthieu Koepf, Karin J. Young, Christian F. A. Negre, Laura J. Allen, William R. McNamara, Hee-eun Song, Victor S. Batista, Robert H. Crabtree, and Gary W. Brudvig*

Department of Chemistry, Yale University, P. O. Box 208107, New Haven, CT 06520-8107

[†]*Department of Chemistry and Materials Science Program, University of New Hampshire, Durham, New Hampshire 03824, United States*

[*]E-mail Addresses: gary.brudvig@yale.edu

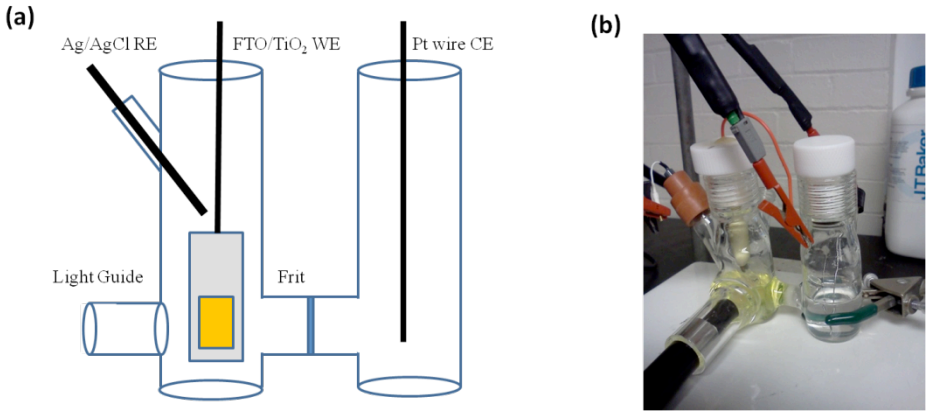

Figure S1. (a) The schematic and (b) a picture of the home-built PEC cell used in this study.

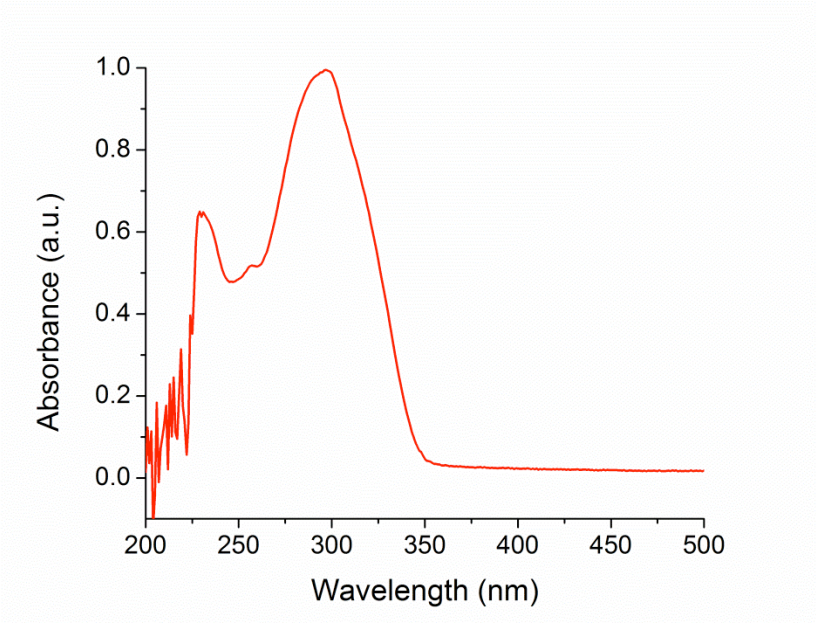

Figure S2. UV–vis spectrum of **L** in dichloromethane solution. Notably, there is no absorbance in the visible region.

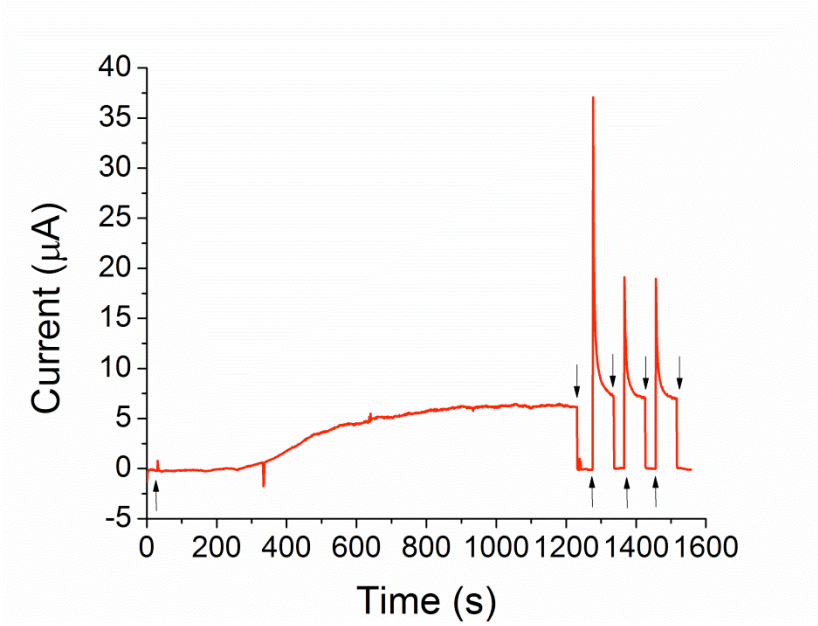

Figure S3. Photoelectrochemical response of Mn^{II}–**L**–TiO_2 with multiple light-on/light-off cycles. Up and down arrows indicate times when the light was turned on and off, respectively.

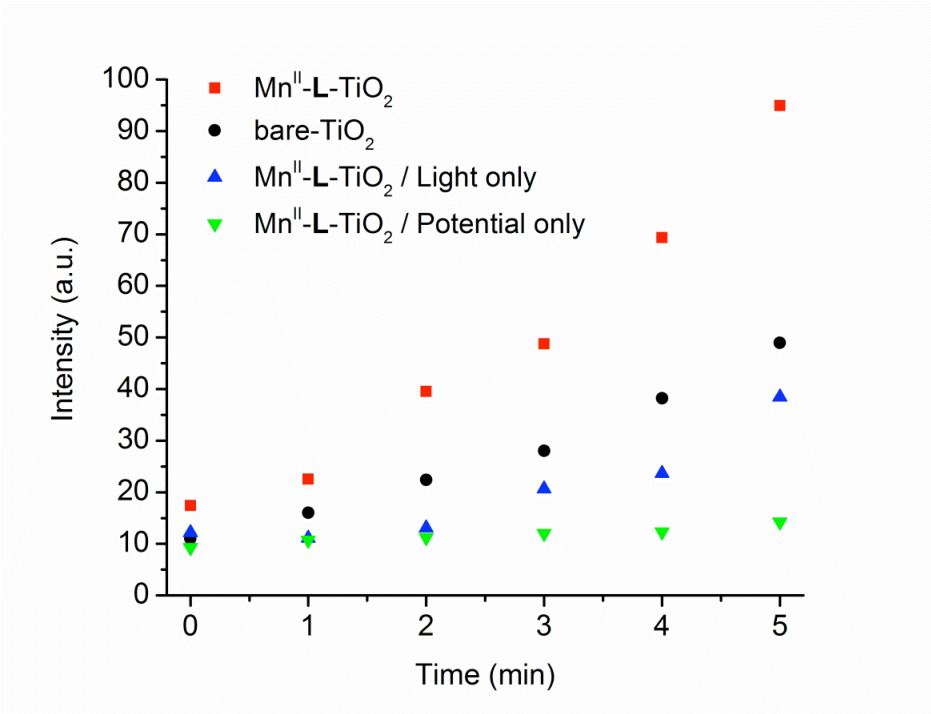

Figure S4. Integrated fluorescence intensity of aliquots taken from photoelectrolysis cell under different anode conditions: fully-assembled Mn^{II} –**L**–TiO$_2$ (red squares), bare TiO$_2$ (black circles), Mn^{II} –**L**–TiO$_2$ anodes disconnected from the circuit (blue triangles), and Mn^{II} –**L**–TiO$_2$ anodes not exposed to light (green triangles).

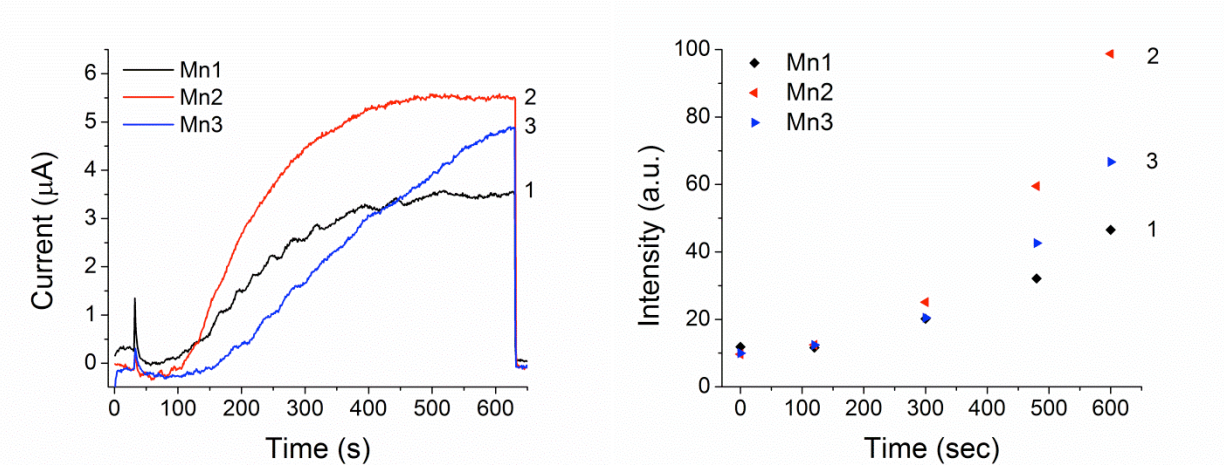

Figure S5. Comparison of photoelectrochemical response and fluorescence intensity for three Mn^{II}–**L**–TiO$_2$ photoanodes. Photocurrents roughly correspond to integrated fluorescence intensity.

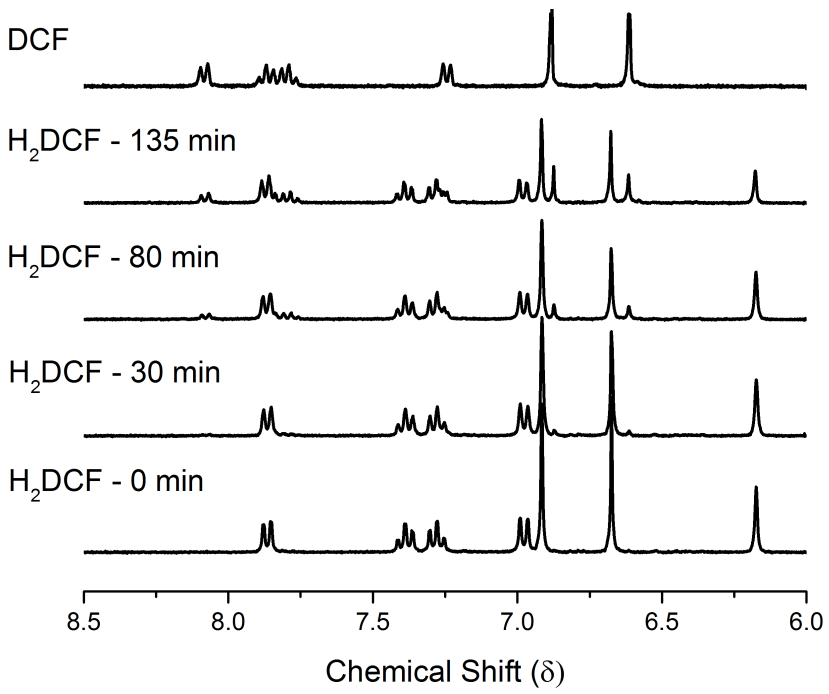

Figure S6. Normalized ^{1}H NMR spectra of H_2DCF in aerated CD_3OD/D_2O solution following photolysis. The H_2DCF sample shows clean conversion to DCF under these conditions. A pure sample of DCF was included for comparison.

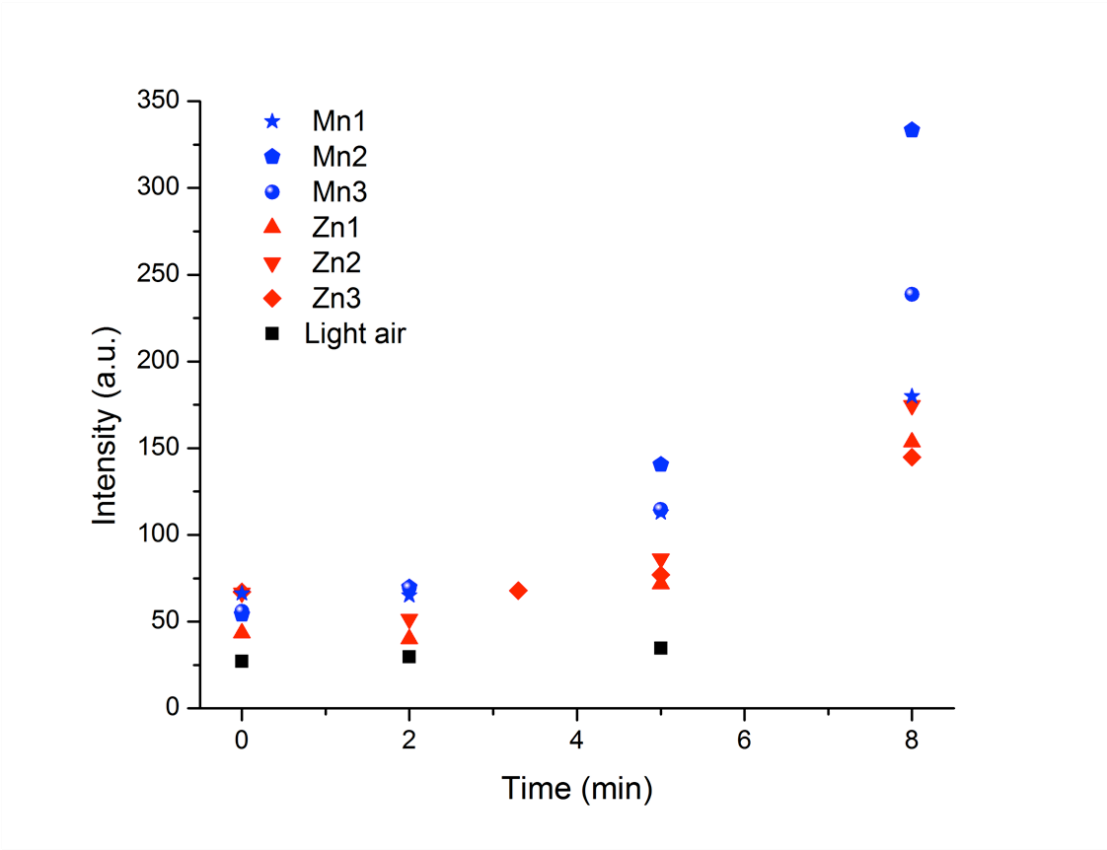

Figure S7. Integrated fluorescence intensity of solutions prepared from aliquots of 20 μM solutions of H_2DCF solutions undergoing visible-light photoelectrolysis with Mn^{II}–**L**–TiO_2 (red circles) or Zn^{II}–**L**–TiO_2 (blue squares) anodes.

Kinetic Model

We consider photoexcitation of an adsorbate molecule covalently bound to a semiconductor surface, a process that promotes an electron in the adsorbate from the ground to the excited state. We assume that the photoexcited state is isoenergetic with an electronic state in the semiconductor conduction band, inducing IET (see Fig. 5 of the manuscript).

The effective rate constant for electron injection is $k_{inj} = [p]k_{inj}^{*}$, where [p] is the effective concentration of photons as determined by the light intensity. The injection is typically ultrafast and is followed by forward electron transfer from terpyridine (T) to phenylacac (A), evolving the system from [1] to [2] with rate constant k_{12} and backward, from [2] to [1], with rate constant k_{21}. In addition, we assume that the hole left in the terpyridine ligand oxidizes Mn^{2+} to Mn^{3+} with an oxidation rate constant k_{23} and recombination k_{32}. Furthermore, [3] could recombine into [0] directly with rate constant k_r. We assume $k_{23} >> k_{32}$ to ensure a chemically sensible model, where Mn is rapidly oxidized by a hole localized in the phenylterpyridine ligand.

2. Quantitative Analysis of the EPR Signal

We find the rate constants k_{12} and k_{21} by considering the slow kinetics, monitored by EPR, after the initial pre-equilibrium of Mn^{II}-T-A-TiO_2 and Mn^{II}-T-A^{h+}-TiO_2^{e-} established by ultrafast injection and recombination:

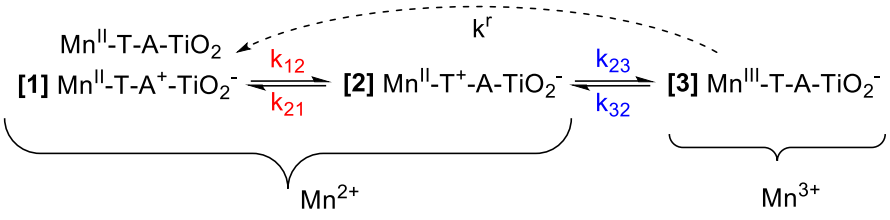

Figure S8. Schematic of the slow kinetics monitored by EPR, after the initial pre-equilibrium established, by ultrafast injection and recombination upon turning the light on.

According to Fig. S7, the kinetics equations are:

$$\frac{d[1]}{dt} = -k_{12}[1] + k_{21}[2] + k_r[3]$$
$$\frac{d[2]}{dt} = k_{12}[1] - k_{21}[2] - k_{23}[2] + k_{32}[3] \qquad (3)$$
$$\frac{d[3]}{dt} = k_{23}[2] - (k_{32} + k_r)[3]$$

When p(0)=[1]+[2]+[3], we obtain:

$$\frac{d[1]}{dt} = -k_{12}[1] + k_{21}(p(0) - [1] - [3]) + k_r[3]$$
$$\frac{d[3]}{dt} = k_{23}(p(0) - [1] - [3]) - (k_{32} + k_r)[3] \qquad (4)$$

with

$$\frac{d[1]}{dt} = -k_{11}[1] + k_{13}[3] + k_{21}p(0)$$
$$\frac{d[3]}{dt} = -k_{33}[3] + k_{31}[1] + k_{23}p(0) \qquad (5)$$

where $k_{11}=k_{21}+k_{12}$, $k_{13}= k_r-k_{21}$, $k_{33}=k_r+k_{32}+k_{23}$, and $k_{31}=-k_{23}$.

Solving for [1], from Eq. (5), we obtain:

$$[1] = k_{31}^{-1}\frac{d[3]}{dt} + k_{31}^{-1}k_{33}[3] - k_{31}^{-1}k_{23}p(0)$$
$$\frac{d[1]}{dt} = k_{31}^{-1}\frac{d^2[3]}{dt^2} + k_{31}^{-1}k_{33}\frac{d[3]}{dt} \qquad (6)$$
$$= -k_{11}k_{31}^{-1}\frac{d[3]}{dt} + (k_{13} - k_{11}k_{31}^{-1}k_{33})[3] + (k_{21} + k_{11}k_{31}^{-1}k_{23})p(0)$$

Associating terms, we obtain:

$$\frac{d^2[3]}{dt^2} + (k_{33} + k_{11})\frac{d[3]}{dt} + (k_{11}k_{33} - k_{13}k_{31})[3] - (k_{31}k_{21} + k_{11}k_{23})p(0) = 0 \tag{7}$$

or

$$\frac{d^2[3]}{dt^2} + A\frac{d[3]}{dt} + B[3] - C = 0 \tag{8}$$

with $A = k_{33}+k_{11}$, $B=k_{33}k_{11}-k_{13}\,k_{31}$ and $C=(k_{11}k_{23}+k_{31}k_{21})p(0)$, with solution

$$[3] = A_1 e^{-k^{(+)}t} + A_2 e^{-k^{(-)}t} + \frac{C}{B} \tag{9}$$

where

$$k^{(\pm)} = \frac{A \pm \sqrt{A^2 - 4B}}{2} \tag{10}$$

with $A= k^{(-)}+k^{(+)}$ and $B= k^{(-)}k^{(+)}$.

We note that for the case of light OFF, $k_{inj} = 0$ since [p] = 0. In addition, $[Mn^{II}\text{-T-}A^{h+}\text{-}TiO_2^{e-}] = 0$, since the transition from $[Mn^{II}\text{-T-}A^{h+}\text{-}TiO_2^{e-}]$ to $[Mn^{II}TATiO_2]$ is ultrafast. Therefore, the resulting kinetic model is analogous to the light-on model but with an effective kinetic constant $k_{12} = 0$:

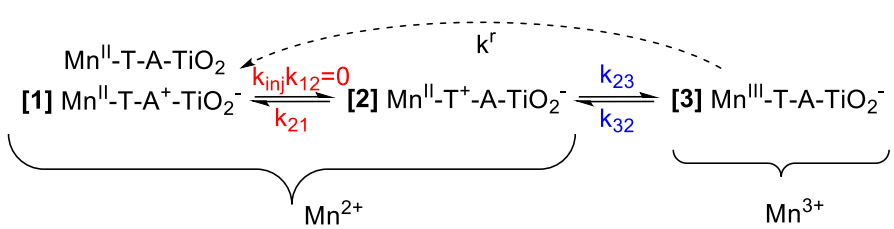

Figure S9. Schematics of the slow recombination kinetics monitored by EPR after turning the light off.

For the case of light OFF (k_{12}=0), $k^{(-)OFF}$= (42.16 s)$^{-1}$ and $k^{(+)OFF}$ = (9.18 s)$^{-1}$, while for light ON, we obtain $k^{(-)OFF}$= (14.1 s)$^{-1}$ and $k^{(-)OFF}$ = (3.0 s)$^{-1}$.

Assuming that $k_{23} >> k_{32} \approx 0$, we solve for k_r and k_{23}, giving:

$$\begin{aligned} k_{23} &= \frac{(k^{(-)OFF} + k^{(+)OFF})\, k_{21} - k_{21}^2 - k^{(-)OFF} k^{(+)OFF}}{k_{21}} \\ k_r &= \frac{k^{(-)OFF} k^{(+)OFF}}{k_{21}} \end{aligned} \tag{11}$$

For the case of light-on, we have $k^{(-)ON}$=(14.11 s)$^{-1}$ and $k^{(+)ON}$=(3.04 s)$^{-1}$, and solving for k_{12} and k_{21}, we obtain:

$$\begin{aligned} k_{12} &= (k^{(-)ON} + k^{(+)ON}) - (k^{(-)OFF} + k^{(+)OFF}) \\ k_{21} &= \frac{\left(k^{(-)OFF}\right)^2 + \left(k^{(-)OFF} + k^{(+)OFF}\right)\left(k^{(+)OFF} - k^{(+)ON} - k^{(-)ON}\right) + k^{(-)ON} k^{(+)ON}}{k^{(-)OFF} + k^{(+)OFF} - k^{(-)ON} - k^{(+)ON}} \end{aligned} \tag{12}$$

giving k_{12}=0.272 s^{-1} and k_{21} = 0.0546 s^{-1} (*i.e.*, $K_1 \approx 5$, as indicated in Sec. 1). Substituting these values into Eq. (11) we obtain, k_{23}=0.0307 s^{-1} and k_r = 0.0472 s^{-1}.

We obtain [3] as a function of time by using Eq. (9), with parameters given in Table 1, with A_1 and A_2 obtained by making [3]=[2]=0 at t=0. We solve for [2], as a function of [3], from Eq. (3), and for [1] as a function of [3] from p(0)=[1]+[2]+[3]. Figure S11 shows [1], [2] and [3] as a function of time.

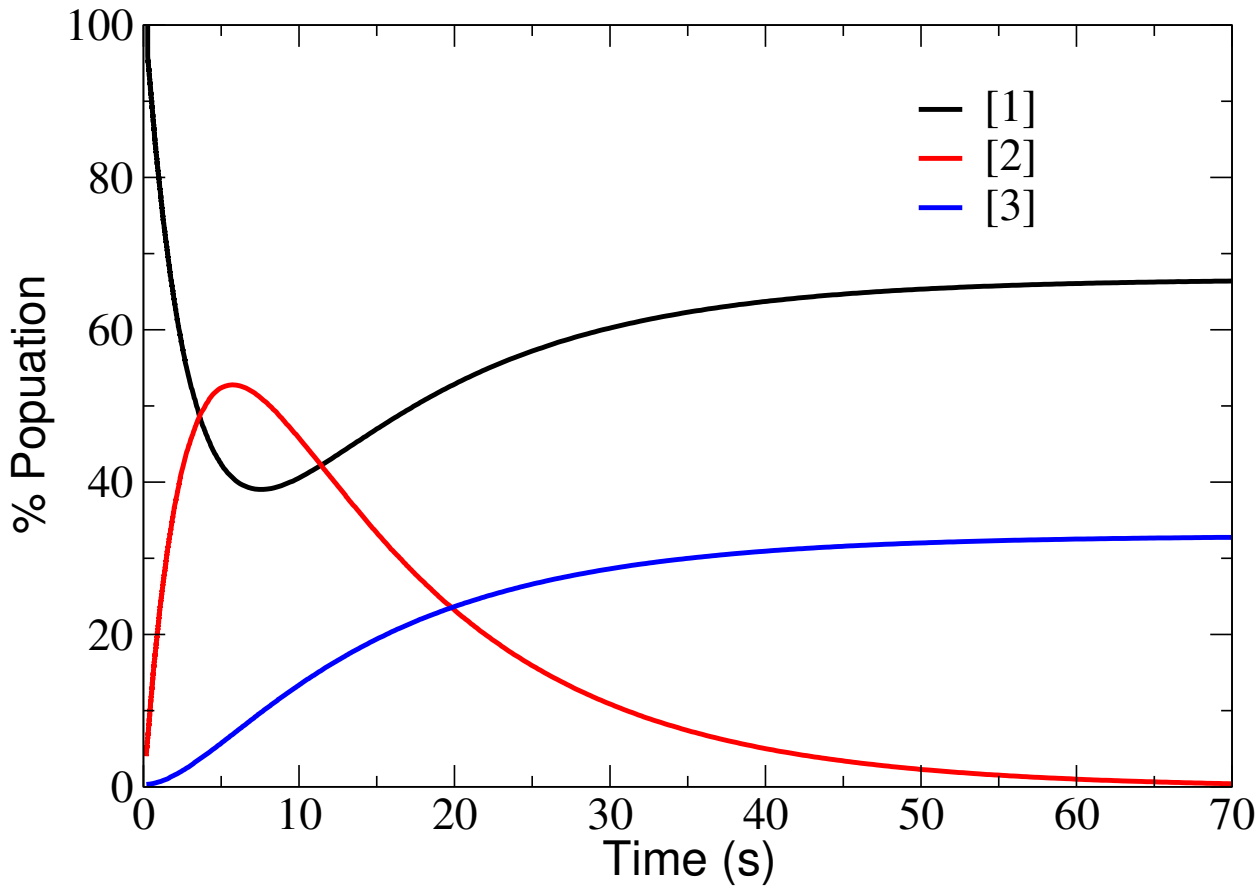

Figure S10. Populations of [1], [2] and [3] as a function of time.